LAMINAR VAPOR FLOW IN A HEAT PIPE

Ya. S. Kadaner and Yu. P. Rassadkin

UDC 536.248.2

Laminar vapor flow in the evaporation, adiabatic, and condensation sections of a heat pipe is considered. The problem is solved by using a parametric method. The solution resulted in a graphoanalytical method of determining the vapor-pressure loss in all sections of the pipe.

Because of their high reliability, autonomy, and capacity to transmit large heat fluxes, heat pipes are being used more and more in various branches of engineering. In a number of cases, heat pipes are required which operate at relatively low temperatures, where the heat carriers are low-boiling-point fluids such as water and ethanol. The vapor flow in all sections of the pipes hence turns out to be laminar. The vapor-pressure losses in the separate sections must be known to determine the thermal power transmitted by the pipe. As is known, a heat pipe consists of an evaporation section, a transfer section, and a condensation section. The evaporation and condensation sections can be considered pipes with porous walls through which vapor injection and suction, respectively, are accomplished. The end-face walls and the walls of the transfer section are impermeable. A number of authors [1-6] has investigated the problem of gas flow in a pipe with injection and suction. Thus, in [1-3] the system of equations describing incompressible fluid flow in a pipe with injection at the wall by using a particular dependence of the stream function

$$\psi = \left[A + B\frac{x}{R}\right] f\left(\frac{r}{R}\right)^2,$$

reduces to an ordinary differential equation which is solved for $\mathrm{Re_w}$ by the method of small perturbations for $|\mathrm{Re_w}| \gg 1$ and $|\mathrm{Re_w}| \ll 1$, and the solution is later extended to the whole range of $\mathrm{Re_w}$ numbers, which does not have any foundation because of the poor convergence of the series. The solution obtained in [2] for small and large injection numbers $\mathrm{Re_w}$ is extended to a flow with suction, which is not valid, since, as has been remarked in [3, 4], the numerical solution of the initial equation, as well as experimental investigations, show that the velocity profile for large suction numbers $\mathrm{Re_w}$ is different from that which is presented in [4]. The papers [5, 6] are devoted to a theoretical study of the influence of the establishment of hydrodynamic stabilization on friction on the condensation and evaporation sections in a pipe with suction. The problem is solved in these papers by a parametric method, whose crux is that the axial velocity is sought as a known function of the radial coordinate with coefficients dependent on the coordinate axes. The advantage of this method is relative simplicity and good accuracy. Among the disadvantages of these papers should be the polynomial representation which, as the authors themselves remark, describes the velocity profile poorly in a number of cases. Also without foundation is the use of differential together with integral characteristics to find the unknown coefficients, which can result in false results, as the investigation noted in [7, 8] showed.

Under the assumption of incompressibility of the vapor, constant normal injection and suction along the length on the pipe wall, and constancy of the pressure along the pipe radius, the system of equations describing the vapor flow is the following:

$$u\frac{\partial u}{\partial x} + v\frac{\partial u}{\partial r} = -\frac{1}{\rho}\cdot\frac{\partial P}{\partial x} + \frac{\nu\partial}{r\partial r}\left(r\frac{\partial u}{\partial r}\right),$$

$$\frac{\partial u}{\partial x} + \frac{1}{r}\cdot\frac{\partial (vr)}{\partial r} = 0, \quad \frac{\partial P}{\partial r} = 0 \tag{1}$$

Translated from Inzhenerno-Fizicheskii Zhurnal, Vol. 28, No. 2, pp. 208-216, February, 1975. Original article submitted April 10, 1974.

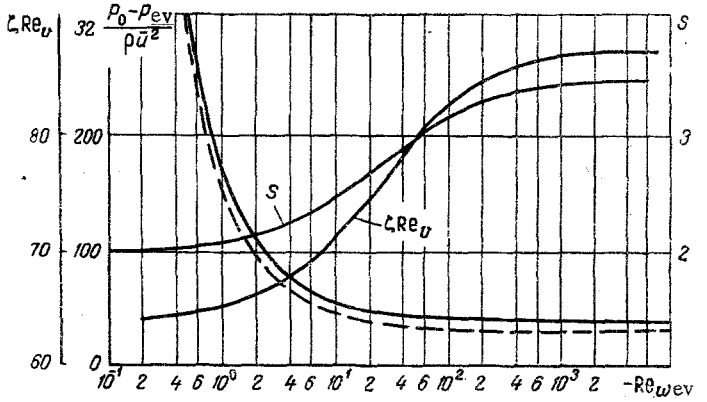

Fig. 1. Dependence of the friction coefficient and pressure loss on the number Re_{wev} on the evaporation section (dashed curve is results of a computation for $\zeta RE_v = 64$).

with the boundary conditions:

a) evaporation section,

$$r = 0 \quad \partial u/\partial r = 0;$$

$$r = d/2 \quad u = 0, \quad v = -v_w, \quad x = 0 \quad u = 0, \quad P = P_0;$$

b) transfer section,

$$r = d/2 \quad u = 0, \quad v = 0; \quad x = l_{ev} P = P_{eev}, \quad u = u_{eev};$$

c) condensation section,

$$r = d/2 \quad u = 0, \quad v = v_w; \quad x = l_{ev} + l_t = u_{et}, \quad P = P_{et}.$$

After insertion of the dimensionless functions and coordinates $X = x/d$, $r' = 2r/d$, $u' = u/v_W$, $P' = 2P/\rho v_W^2$ and elimination of the radial velocity on the evaporation section, by omitting the prime on the variables, the system of equations (1) and the boundary conditions become

$$2\int_0^1 urdr = 4X,$$

$$u\frac{\partial u}{\partial X} - \frac{1}{r}\frac{\partial u}{\partial r}\int_0^r \frac{\partial u}{\partial X} rdr = -\frac{1}{2}\frac{dP}{dX} - \frac{4}{Re_{wev}}\frac{1}{r}\frac{\partial}{\partial r}\left(r\frac{\partial u}{\partial r}\right), \tag{2}$$

$$r = 0 \quad \frac{\partial u}{\partial r} = 0; \quad r = 1 \quad u = 0; \quad X = 0 \quad u = 0, \quad P = 2P_0/\rho v_w^2.$$

Here $Re_{wev} = -v_W d/\nu < 0$. Let us solve (2) by the parametric method elucidated in [7, 8], for which we seek the axial velocity profile in the form

$$u = u_e(1 - r^s), \tag{3}$$

where $u_e = u_e(X)$; $s = s(X)$ and the unknown functions u_e, s, P are found from the following integral equations:

$$\frac{d}{dX}\int_0^1 u^2 rdr = -\frac{1}{4}\cdot\frac{dP}{dX} - \frac{4}{Re_{wev}}\cdot\frac{\partial u}{\partial r}\Big|_0^1;$$

$$\frac{d}{dX}\int_0^1 \frac{1}{r}\int_0^r u^2 rdrdr - \int_0^1 \frac{u}{r}\int_0^r \frac{\partial u}{\partial X} rdrdr = \frac{1}{8}\cdot\frac{dP}{dX} - \frac{4u}{Re_{wev}}\Big|_0^1; \tag{4}$$

$$2\int_0^1 urdr = 4X.$$

Substituting (3) into (4) and integrating, we obtain the system of equations

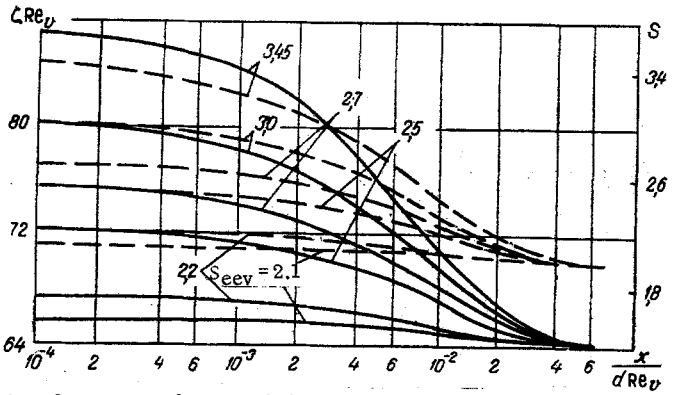

Fig. 2. Dependence of the change in friction coefficient along the length of the transfer section (solid curves are for $\zeta \mathrm{Re}_v$ and dashes for s).

$$\frac{ds}{dX} = -\frac{(s+2)(s-1)^3}{X(s^2-6s-7)}\left[\frac{s^2-2s-5}{2(s+1)^2} - \frac{2}{\mathrm{Re}_{wev}}\frac{s^2-4}{s}\right],$$
$$\frac{dP}{dX} = -64X\left[\frac{s+2}{s-1} - \frac{X}{2(s+1)^2}\frac{ds}{dX} - \frac{s+2}{\mathrm{Re}_{wev}}\right] \quad (5)$$

with the boundary conditions

$$X = 0 \quad P = 1; \quad s = s_0.$$

The axial velocity profile is

$$u = 4X\frac{s+2}{s}(1-r)^s, \quad (6)$$

and the local friction coefficient is

$$\zeta = -\frac{16\left.\frac{\partial u}{\partial r}\right|_{r=1}}{\mathrm{Re}\rho\bar{u}^2} = \frac{16(s+2)}{\mathrm{Re}_v}; \quad \mathrm{Re}_v = -4X\mathrm{Re}_{wev}.$$

It can be assumed that the radial velocity at the entrance to the evaporation section depends only on the radial coordinate, and the axial velocity profiles presented in [2] can be used to determine the parameter s_0. This assumption is not valid in direct proximity to the end-face wall of the evaporator section of the heat pipe, where eddy zones can exist and the elucidated parametric method is not applicable. But as exact computations and the experiments of some authors [9] show, this hypothesis can already be used at a range of one caliber from the end-face wall.

From the condition that the integrated motion pulse and the discharge are constant for the velocity profile (3) and from [2], it is possible to determine s_0 as a function of the number Re_{wev}

$$s_0 = \frac{2}{2(1+0.0278\,\mathrm{Re}_{wev}-0.00384\,\mathrm{Re}_{wev}^2)-1} \text{ for } |\mathrm{Re}_w| < 1,$$
$$s_0 = \frac{2}{\left(1-\frac{2}{\mathrm{Re}_{wev}}-\frac{4{,}43}{\mathrm{Re}_{wev}^2}\right)-1} \text{ for } |\mathrm{Re}_w| > 1.$$

Solving the system of equations (5), the dependences S(X), P(X), and the friction coefficient can be determined.

The parametric method elucidated was used to solve a numerous class of heat-exchange and friction problems for laminar fluid and gas flow in a circular pipe. The results of computations were compared with known exact solutions and showed not more than a 5-6% difference in the velocity profiles and not more than a 3% difference in the friction coefficient.

The solution of the system (5) for the range $0.5 > \mathrm{Re}_{wev} > -10^4$ and $0.2 < X < 100$ showed that the parameter s tends to its asymptotic value, dependent on the number Re_{wev}, quite rapidly. Therefore,

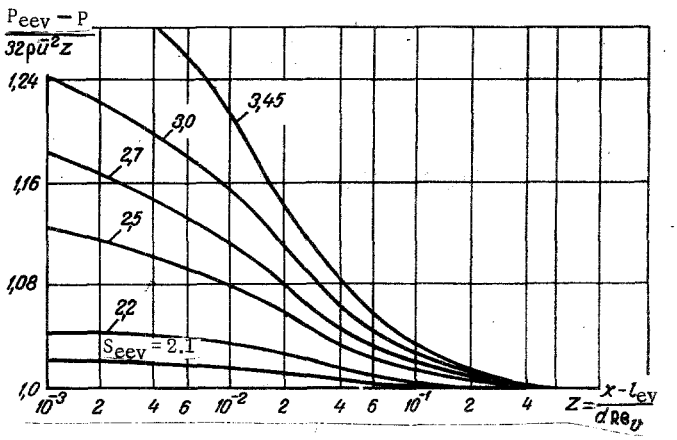

Fig. 3. Dependence of the change in pressure loss along the length of the transfer section.

stream stabilization sets in quite rapidly along the length of the evaporation section. A comparison between the velocity profiles and the data presented in [2] showed that the difference does not exceed 1-2%. Since vapor flow along the length of the evaporation section remains similar, i.e., ds/dX = 0, then the following simple expressions are obtained to determine s and P:

$$\mathrm{Re}_{wev}=\frac{4(s^2-4)(s+1)^2}{s(s^2-2s-5)};$$
$$\frac{P_0-P}{\frac{\rho v_w^2}{2}}=32X^2\left(\frac{s+2}{s+1}-\frac{s+2}{\mathrm{Re}_{wev}}\right). \tag{7}$$

The self-similarity on the evaporation section can be explained by the fact that the injection velocity on the wall agrees in direction with the radial velocity component, which results in an increase in boundary-layer thickness and rapid stream stabilization. This deduction about the strong laminarization of the stream is confirmed by the experiments of a number of authors. An analysis of (7) shows that $s \to 2$ and $\zeta\mathrm{Re}_V \to 64$ as $\mathrm{Re}_{wev} \to 0$ and $s \to 3.45$ and $\zeta\mathrm{Re}_V \to 87.2$ as $\mathrm{Re}_{wev} \to -\infty$. This corresponds, with high accuracy, to axial velocity profiles in the corresponding limit cases $U = 8X(1 - r^2)$ and $U = 2\pi X\cos(\pi/2)r^2$. Presented in Fig. 1 are the computed dependences of the quantities s, $\zeta\mathrm{Re}_V$, the relative pressure losses $32[(P_0 - P)/\rho\bar{u}^2]$ as a function of the injection Re_{wev}. Presented there for comparison are the pressure losses computed for the case with injection for $\zeta\mathrm{Re}_V = 64$. It is seen that the difference between the curves does not exceed 10-12%.

The vapor flow in the transfer section of a heat pipe is determined by the shape of the axial velocity profile at the entrance to this section and is described by the following equation:

$$u\frac{\partial u}{\partial Z}-\frac{1}{r}\cdot\frac{\partial u}{\partial r}\int_0^r\frac{\partial u}{\partial Z}r\,dr=-\frac{1}{2}\cdot\frac{dP}{dZ}+\frac{4}{r}\cdot\frac{\partial}{\partial r}\left(r\frac{\partial u}{\partial r}\right) \tag{8}$$

and the boundary conditions

$$r=0\ \frac{\partial u}{\partial r}=0;\quad r=1\ \ u=0;\quad Z=0\ \ u=u_{eev};\ P=2P_0/\rho\bar{u}^2.$$

Here

$$Z=\frac{x-l_{ev}}{d\,\mathrm{Re}_v};\quad r=\frac{2r'}{d};\quad u=\frac{u'}{\bar{u}};\quad P=\frac{2P_{eev}}{\rho\bar{u}^2};\quad \mathrm{Re}_v=\frac{\bar{u}d}{\nu}.$$

The solution of (8) is presented in [8], where the axial velocity profile is sought in the form $u = [(s + 2)/s](1 - r^s)$ and s and P are found from the system of equations

$$\frac{ds}{dZ}=8\frac{(s+2)^2(s+1)^3(s-2)}{s(s^2+6s+7)},$$
$$\frac{dP}{dZ}=-2\left[8(s+2)-\frac{1}{(s+1)^2}\frac{ds}{dZ}\right] \tag{9}$$

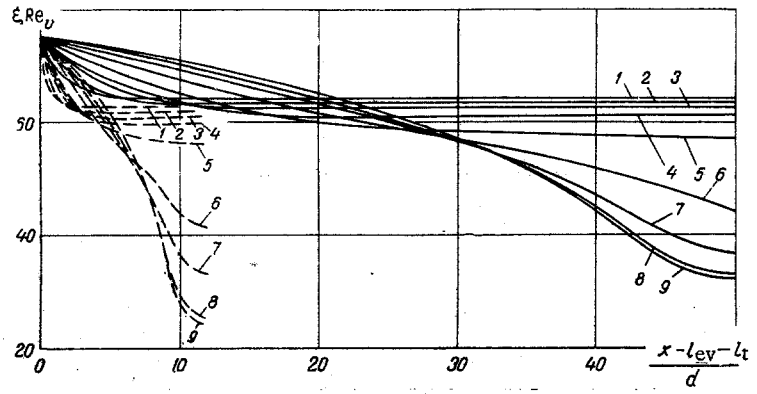

Fig. 4. Dependence of the change in friction coefficient along the length of the condensation section for $s_{et} = 2.1$ (dashed curves for $l_c/d = 10$ and continuous curves for $l_c/d = 50$): 1) $Re_{wc} = 1$; 2) 1.5; 3) 2; 4) 3; 5) 5; 6) 10; 7) 20; 8) 50; 9) 100.

with the boundary conditions $Z = 0$, $P = 1$; $s = s_{eev}$. Since the entrance profile on the transfer section is the exit profile in the evaporation section, then s_{eev} varies between $2 < s_{eev} < 3.45$ for $0 > Re_{wev} > -\infty$.

The results of computing the parameter s, the friction coefficient ζRe_v, and the pressure loss along the pipe length are presented in Figs. 2 and 3 for different values of s_{eev}. It is seen from the graphs in these figures that as the fullness of these profiles increases, i.e., as $|Re_{wt}|$ increases, the friction coefficient, the pressure loss, and the initial section of hydrodynamic stabilization increase.

Vapor flow on the condensation section is described by the following equation:

$$u\frac{\partial u}{\partial X} - \frac{1}{r}\int_0^r \frac{\partial u}{\partial X}\, r dr = -\frac{1}{2}\cdot\frac{dP}{dX} + \frac{4}{Re_{wc}}\,\frac{1}{r}\cdot\frac{\partial}{\partial r}\left(r\frac{\partial u}{\partial r}\right) \qquad (10)$$

with the boundary conditions

$$r = 0 \quad \frac{\partial u}{\partial r} = 0; \quad r = 1 \quad u = 0; \quad X = l_{ev} + l_t \quad u = u_{et}; \quad P = \frac{2P_{et}}{\rho v_w^2}.$$

If we go over to a new axial coordinate $y = l/d - X$, then by using the parametric method elucidated above to solve (10), we obtain a system of equations (5) with appropriate boundary conditions,

$$y = 0 \quad s = s_{et}, \quad P = 2P_{et}/\rho V_w^2,$$

to determine the unknown functions s and P, where $Re_{wc} > 0$.

Since the condensation section can be either directly behind the evaporation section or the transfer section, then the entrance profile on the condensation section is the exit profile on the transfer or evaporation sections. Hence, s_{et} can vary between 2 and 3.45, which corresponds to the two limit cases at the entrance to the condensation section: stabilized for $s_{et} \to 2$, which can be realized either for low injection numbers Re_{wev} in the evaporation section, or for long lengths of the transfer section, and $s_{et} \to 3.45$ corresponds to the velocity profile when $Re_{wev} \to -\infty$.

The system of equations (5) was solved for a broad range of variation of the parameters Re_{wc}, s_{et} and l_c/d.

Computations showed that the parameter s diminishes along the pipe length from s_{et} to a value governed by the number Re_{wc}, where when $Re_{wc} \to \infty$, $s \to 0$.

Presented in Fig. 4 are results of computations of the local friction coefficient for different values of l_c/d, Re_{wc}. The computations show that the initial section of hydrodynamic stabilization can occupy a significant part of the length of the condensation section, depending on s_{et} and Re_{wc}.

For $Re_{wc} < 3$ the initial stabilization section occupies approximately one-third the whole length of the condensation section, and practically the whole length for $3 < Re_{wc} < 20$ for any values $2 < s_{et} < 3.45$ and $10 < l_c/d < 100$.

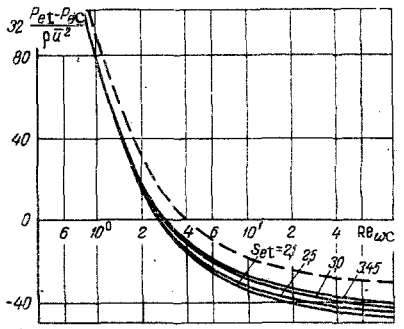

Fig. 5. Dependence of the pressure loss on Re_{wc} in the condensation section (dashed curve is results of a computation for $\zeta Re_v = 64$).

Flow stabilization at some length at the end of the condensation section is observed when $Re_{wc} > 20$. These computational results can be explained by the fact that the direction of the suction velocity at the pipe wall is opposite to the direction of the stream radial velocity component which characterizes the boundary-layer formation. These two factors influence the shaping of the axial velocity profile oppositely, where the factor of an increase in boundary-layer thickness is predominant for low Re_{wc}, and the pressure drops along the length of the section. Both factors are apparently approximately identical for the numbers $3 < Re_{wc} < 20$, and as has been remarked on in [4, 5], the stream becomes unstable, and the hydrodynamic stabilization section can occupy the whole length. In this case (6) does not describe the velocity profile with the sign-varying curvature; hence, it is impossible to say anything about the presence of separation flows on the basis of the parametric method.

Suction predominates over the increase in boundary-layer thickness in the case $Re_{wc} > 20$, the vapor pressure along the length rises, and hydrodynamic stabilization sets in at some length, i.e., the flow becomes self-similar. Computations show that $s \to 0$ as $Re_{wc} \to \infty$ and resolving the indeterminacy in the expression for the axial velocity profile (6) yields

$$\lim_{s\to 0}\left[\left(\frac{l_c}{d}-X\right)\frac{s+2}{s}(1-r^s)\right]=\lim_{s\to 0}\left[\left(\frac{l_c}{d}-X\right)\right.\left.[1-r^s-(s+2)r^s\ln r)=-8\left(\frac{l_c}{d}-X\right)\ln r.\right.$$

The friction coefficient varies, correspondingly, between 87.2 and 32. It must be noted that stream turbulization at the pipe wall can start earlier as the suction increases, than for flow in a pipe with impermeable walls. Hence, the computations expounded above for high numbers can be used for a small entrance neighborhood.

Results of computations of the pressure loss along the length of the condensation section showed that the quantity $32(P_{et} - P_{ec})/\rho\bar{u}^2$ depends only on the parameter s_{et} and the number Re_{wc}, which affords the possibility of constructing a universal graph of the dependence of the pressure loss on the numbers Re_{wc} and s_{et} (Fig. 5). Presented there for comparison are results of computations for $\zeta Re_v = 64$, which show that the difference can reach 30%. Hence, pressure recovery occurs on the condensation section for $Re_{wc} > 3$.

On the basis of the equality of the vapor discharge through both heat-pipe sections, it follows that in the transfer section

$$Z=\frac{l_t}{d\,Re_{vt}};\quad \bar{v}_t=-4\frac{l_{ev}}{d}v_w;\quad Re_{vt}=-4\frac{l_{ev}}{d}Re_{wev}\quad P_t=\frac{P_{ev}}{16\left(\frac{l_{ev}}{d}\right)^2},\tag{11}$$

and in the condensation section

$$Re_{wc}=-\frac{l_{ev}}{l_c}Re_{wev};\quad P_c=P_{ev}\left(\frac{l_c}{l_{ev}}\right)^2.\tag{12}$$

The results obtained, presented in Figs. 1-3 and 5, can be used to compute the pressure loss in the individual sections of the heat pipe. The method of computing the pressure loss reduces to the following for given values l_{ev}, l_t, l_c, d, G, P_0 of the physical properties of the vapor.

1. The Re_{wev} on the evaporation section is calculated and the values of the parameter s and the pressure loss are determined from the graph in Fig. 1.

2. The Re_{vt} and Z in the transfer section for which the quantity s_{et} and the pressure loss are determined from the graphs in Figs. 2 and 3 for given s_{ev} and Z are calculated from relations (11).

3. The Re_{wc} is determined in the condensation section by means of (12), and then the pressure drop is found for given s_{et}, Re_{wc}, l_c/d from the graph in Fig. 5.

Therefore, this method permits the determination of the vapor-pressure losses in separate sections of a heat pipe with the influence at the entrance to each section taken into account.

NOTATION

x, $X = x/d$, $Z = x/dRe_{0t}$	is the axial coordinate;
r	is the radial coordinate;
d	is the diameter of the vapor channel;
l_t, l_{ev}, l_c	are the lengths of the evaporation, transfer, and condensation sections, respectively;
l	is the total heat-pipe length;
P and ρ	are the vapor pressure and density;
$Re_{wev} = -Re_{wc} = -V_w d/\nu$, $Re_{0t} = \bar{u}d/\nu$	are the Reynolds numbers on the evaporation, condensation, and transfer sections, respectively;
$\bar{u}$	is the mean mass flow rate;
G	is the vapor discharge.

Subscripts

w	is the pipe wall;
ev	is the evaporation section;
t	is the transfer section;
c	is the condensation section;
0	is the values of the parameters at the entrance to the evaporation section;
eev, et, ec	are the values of the parameters at the exits from the evaporation, transfer, and condensation sections, respectively.

LITERATURE CITED

1. A. S. Berman, J. Appl. Phys., 24, No. 9 (1953).
2. S. W. Yuan and A. B. Finkelstein, Trans. ASME, 78, No. 4 (1956).
3. A. S. Berman, J. Appl. Phys., 27, No. 12 (1956).
4. A. S. Berman, Proc. Intern. Congr. Peaceful Uses of Atomic Energy, 720 (1958).
5. H. L. Weissberg, J. Phys. of Fluids, 2, No. 5 (1959).
6. C. A. Busse, Thermionic Conversion Specialist Conference, Palo Alto, California (1967).
7. Ya. S. Kadaner, Yu. P. Rassadkin, and E. L. Spektor, Inzh.-Fiz. Zh., 20, No. 1 (1971).
8. Yu. P. Rassadkin and E. L. Spektor, Inzh.-Fiz. Zh., 21, No. 4 (1971).
9. W. E. Wageman and F. A. Guevara, Phys. Fluids, 3, No. 6 (1960).